IJIRSET
International Journal of Innovative Research in
SCIENCE | ENGINEERING | TECHNOLOGY

e-ISSN: 2319-8753 | p-ISSN: 2347-6710

INTERNATIONAL JOURNAL OF INNOVATIVE RESEARCH

IN SCIENCE | ENGINEERING | TECHNOLOGY

Volume 11, Issue 12, December 2022

ISSN INTERNATIONAL STANDARD SERIAL NUMBER INDIA

Impact Factor: 8.118

9940 572 462 | 6381 907 438 | ijirset@gmail.com | www.ijirset.com

International Journal of Innovative Research in Science, Engineering and Technology (IJIRSET)

| e-ISSN: 2319-8753, p-ISSN: 2347-6710| www.ijirset.com | Impact Factor: 8.118|

||Volume 11, Issue 12, December 2022||

| DOI:10.15680/IJIRSET.2022.1112002 |

Intracranial Cancer Detection by Mobile Phone Electromagnetic Radiation

Niyazi K. ULUAYDIN*[1], S. Selim SEKER[2]

[1*]Department of Electrical and Electronics Engineering, Bogazici University, 34342 Istanbul, Turkey

[2]Department of Electronics Engineering, Uskudar University, 34662 Istanbul, Turkey

*Correspondent Author

ABSTRACT: Cancer is the topping cause of death only after ischemic heart disease in the world. Among cancers, brain tumors are generally one of the hardest to heal. And among the brain tumors, glioblastoma multiforme, which is a very aggressive intracranial cancer, has one of the highest mortality rates. These cancers are rather difficult to diagnose with the lack of manual diagnosis and very aggressive in their progression the disease, thus a later-stage diagnosis would not be much of a benefit. Therefore, medical doctors require advanced medical imaging techniques such as computed tomography and magnetic resonance imaging for intracranial tumors.

The Covid-19 pandemic has caused a global lockdown and has put an enormous load on the medical system. Any similar pandemic would almost paralyze the medical system. In this study, the authors investigate the possibility of an early-stage detection of glioblastoma multiforme by use of mobile phone electromagnetic radiation. Since cancer tissue contains more blood vessels because of its intrinsic energy needs, external electromagnetic radiation would affect the cancer tissue faster than the normal tissue. The authors build the model by introducing a hypothetical ellipsoid cancer tissue into the IEEE phantom head SAR model. By applying two different levels of external electromagnetic exposure, the simulations seek to find a discriminatory temperature change, which can be detected externally.

KEYWORDS:Cancer Detection, Mobile Phone, Covid-19, Electromagnetic Radiation, Dielectric Properties.

I. INTRODUCTION

Cancer is the second leading cause of death after ischemic heart disease in the world [1]. If one reconsiders the aging factor, cancer may even become the most prominent cause of death. Among the cancers, intracranial ones are hardest to reach by topical, intravenous, and even by surgical methods for medical doctors. Therefore, radiotherapy and thermotherapy are used in concert with other therapeutic medicine [2,3]. To increase the efficacy of these therapies, nanomaterials and laser stimulations are proposed [4,5,6,7,8], some of which modify the Blood Brain Barrier (BBB) and Blood Tumor Barrier (BTB) permeability. Some studies also propose blood conductivity improvements by carbon nanotubes and other metallic nanoparticles to increase the conductivity of tumor tissue [4,7,9,10].

Glioblastoma multiforme (GBM) is a very aggressive intracranial cancer with a very high mortality rate [11]. World Health Organization (WHO) classifies GBM as a grade 4 tumor, which is the most malignant [12]. This cancer usually grows in a star-like (astrocytic) shape and can only metastasize in the brain [3,9,10,11,12,13]. Therefore, it is of utmost importance to detect this cancer in its early stages.GBM may trigger some symptoms based on its location and by its pressure. Abnormal breathing and fluctuating pulse, headaches that persist withoutrelief, motor dysfunction, difficulty in speaking and fetching memories, dizziness,eyesight issues, seizures, and vomiting are common to brain tumors.One may expect to observe the symptoms in the GBM case rather faster than in any other brain tumor, both malignant and benign [10,11,12,13].GBM has lower mitochondrial respiration and higher glycolysis for ATP generation [10,11]. This, in turn, increases glucose needs. That is why, the tumor develops, proliferates, and metastasizes through angiogenesis and vascularization [10,11]. GBM has also different electrical characteristics. Its conductivity and permeability values are higher than other tumors and brain tissue [14].With the coronavirus disease 2019 (COVID-19) virus pandemic, we can observe the enormous load on the medical system overall. Most of the medical staff are busy dealing with COVID-19 patients and the hospitals are releasing other patients to make room for COVID-19 patients. As a result, it is almost impossible to access common medical services, let alone advanced medical imaging.With the social distancing rules and hardened access to medical services, one can foresee the rise in distant medical services after this pandemic. With further expectations of the second and third waves of the pandemic in the upcoming wintermonths, the authors believe

| e-ISSN: 2319-8753, p-ISSN: 2347-6710| www.ijirset.com | Impact Factor: 8.118|

||Volume 11, Issue 12, December 2022||

| DOI:10.15680/IJIRSET.2022.1112002 |

many countries with adopting new principles in health care and social services. On the social side, the social trauma will echo through our near future and people will avoid unnecessary social contact. This further emphasizes the importance of alternative solutions by use of new techniques technology brings forth and new approaches to medical services.The authors propose the use of mobile phones to detect GBM and alike brain tumors in their early stages. But unlike the breast cancer case, the tumor and the tissue's electrical properties are closer to each other [15].

The authors use a mobile phone fixed on the side of the head. A hypothetical tumor in an ellipsoid shape with the size 1x1.6x1 cm a-b-c radii is proposed as early-stage GBM. The authors have modified the IEEE specific absorption rate (SAR) phantom head model with the addition of the GBM tumor. They have simulated the EM thermal effects for mobile phone use in the Finite Element Method (FEM) for two different output levels, in six different depths, and six different lateral positions. The findings on the surface temperature change, normal tissue temperature change, and tumor tissue temperature change are presented. The second group of simulations has been simulated to compare the breast and brain cancer detection scenarios [15].

The rest of the paper is organized as follows: Section 2 describes the bio-EM model and the simulation method; Section 3 presents simulation outputs and results over normal tissue, tumor tissue, and surface temperature changes; Section 4 provides a brief discussion of the results; and finally, Section 5 provides the conclusions.

II. MODEL AND SIMULATION SET-UP

The authors have used the Comsol IEEE SAR phantom head as the base bio-EM model (License No: 17073372). This model has a patch antenna as an EM source (Fig. 1). Then, the GBM tumor is defined in the model. For the permeability, permittivity, and conductivity values of GBM, the authors could not have found exact figures from academia for the target frequency. They used a higher nucleus-to-cytoplasm ratio, thinner cell membrane, and loose connection to basal lamina for higher permittivity values. Likewise, they used smaller cell sizes, higher blood content, and thinner cell membrane for higher conductivity values. Eye vitreous humor has been chosen to mimic the tumor properties. The permeability value is taken as 1. Finally, the metabolic rate of the GBM tumor is set for 20000 W/m3, which is approximately tuned for the elevated tumor temperature of around 1^{o}C [16].

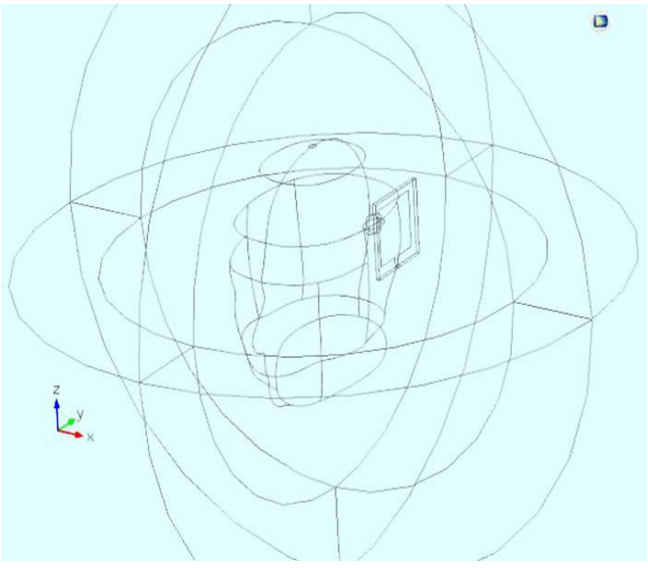

Fig.1.IEEE SAR model with GBM tumor

For the breast case, the same antenna and power figures have been used (Fig. 2) [15]. The metabolic rate of the breast has been set for 450 W/m^3.

| e-ISSN: 2319-8753, p-ISSN: 2347-6710| www.ijirset.com | Impact Factor: 8.118|

||Volume 11, Issue 12, December 2022||

| DOI:10.15680/IJIRSET.2022.1112002 |

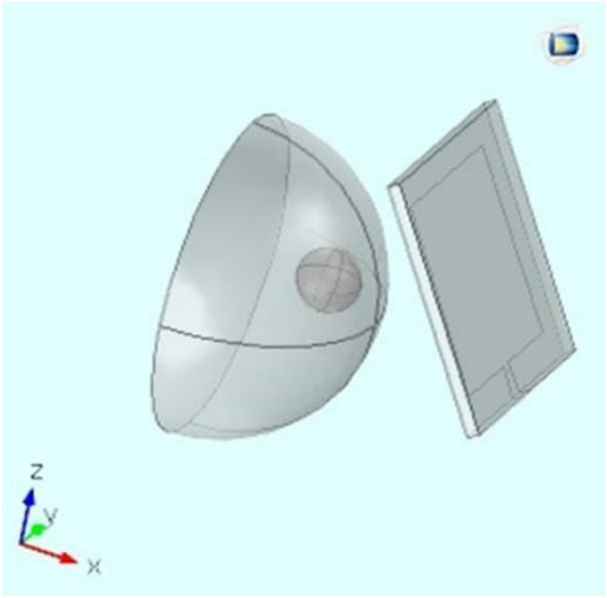

Fig.2. Breast model with tumor.

The brain, the target tumor, and the breast properties are shown in Table 1 with their respectivemetabolic heat values [17-19]. For the rest of the brain, a volumetric interpolation function is used based on M. Levoy's MRI data [20]. The breast tissue is modeled as single tissue with the addition of a spherical tumor with a 1 cm radius[15].Frequency and Property are shown in Table 1.

Table1. Average Permeability, Conductivity, Permittivity, and Metabolic Heat Values for Brain and Tumor at 835 MHZ.

Frequency (835 MHz)	**Property**			
Tissue Type	**Permeability**	**Conductivity**	**Permittivity**	**Metabolic Heat (W/m^3)**
Brain (av.)	1	0.743	46.086	10437
Tumor	1	1.618	68.918	20000
Breast (av.)	1	0.047	5.4351	450

Multiple sets of simulations were conducted with a side EM source on the modified IEEE SAR model using FEM with 835 MHz. The authors have chosen 835 MHz for two clear advantages. 835 MHz frequency or the surrounding band is supported by more than 90% of mobile terminals. Secondly, lower-band mobile telecommunication frequencies have better EM penetration into the tissue.

The simulations have run in the time-dependent set-up for 60 minutes to find temperature saturation times and temperature elevation trends. As for the electromagnetic source, the output is set to be a fixed-power continuous wave from a patch antenna with dimensions 50 mm in length, 50 mm in width, and 2 mm in height [15,21].
The heat transferred by the EM source is calculated by Pennes' Bioheat equation:

$$\rho c \frac{\partial T}{\partial t} = \nabla.(k\nabla T) + \rho Q_{met} + \rho(SAR) - B(T - T_{blood}) \quad (1)$$

where the ρ [kg/m^3] is the material density, c [J/(kg°C)] is the specific heat capacity, k [W/(m°C)] is the thermal conductivity, Q_{met} [W/kg] is the metabolic heat generation rate, B [W/m^3°C] is the blood perfusion coefficient, ω [L/(s·kg)] is the blood perfusion rate, and T_{blood} is blood temperature [22]. The head and breast tissue blood perfusion rates are given in Table 2.

| e-ISSN: 2319-8753, p-ISSN: 2347-6710| www.ijirset.com | Impact Factor: 8.118|

||Volume 11, Issue 12, December 2022||

| DOI:10.15680/IJIRSET.2022.1112002 |

Table 2. Human Head and Breast Tissue Blood Perfusion Rates

Part	Perfusion Rate ((ml/s)/ml)
Brain	$2 \cdot 10^{-3}$
Bone	$3 \cdot 10^{-4}$
Skin	$3 \cdot 10^{-4}$
Breast	$2 \cdot 10^{-4}$

The simulation environment is under standard pressure at 25 ^{o}C, and the base biological temperature is set to zero to represent the fluctuations from the nominal biological base temperature of 37^{o}C. The specific heat capacity of blood is taken as 3639 J/(kg·°C), and the density of blood is taken as 1000 kg/m³ [21].

III. SIMULATION RESULTS

The model (Fig. 1) has been simulated with the EM source at 835 MHz with different tumor depths and positions. Two different power levels have been simulated on the top of a zero-power scenario. Zero power scenario is used to fine tune the tumor metabolism over the normal tissue [16].

The FEM mesh size has been chosen gradually decreasing with the minimum being at the tumor for detailed analysis. As a result, the simulation time has been conservatively prolonged with optimum benefit.

The tissue temperature elevations for lower and higher power levels are depicted in Fig. 3 and 4 for the aligned exposure onto the tumor. The change in tumor maximum temperature profile with depth and with shift on the antenna axis are shown in Fig. 5. The tumor temperature elevations are not mirror symmetrical since the head model is not mirror-symmetrical both shape-wise and tissue-wise. For the lower power scenario, the existence of tumor increases the tissue temperature in a diminishing fashion up to 25 mm. Beyond this point the tumor temperature and the tissue maximum temperature converge to their nominal metabolic elevated temperature and maximum tissue temperature under EM exposure without tumor, respectively (Fig. 3). For the higher power scenario, the existence of tumor increases the tissue maximum temperature in an increasing fashion between 10 to 25 mm (Fig. 4). The higher power exposure increases both tissue and tumor temperature, but the tissue absorbs more power as the tumor is placed deeper (Fig. 6).

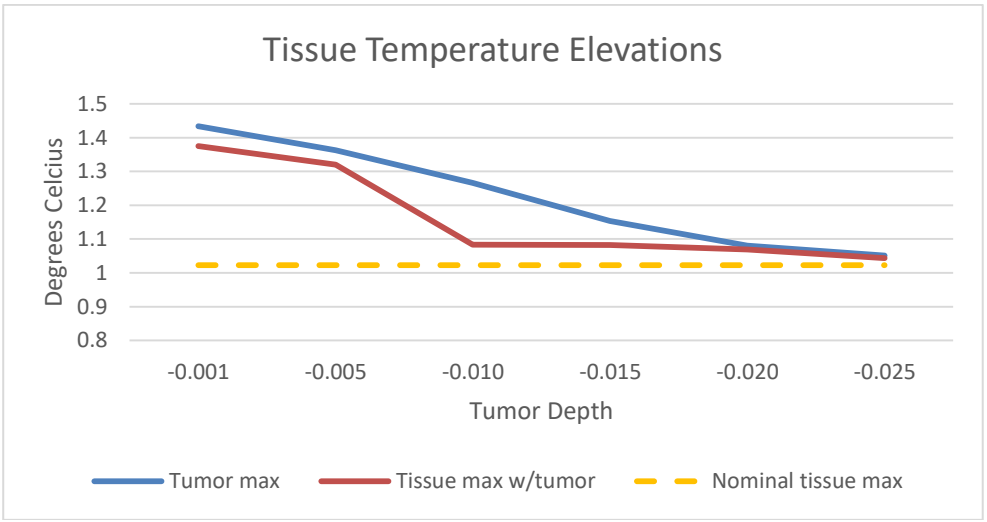

Fig.3. Tissue temperature elevations with changing tumor depth at lower power EM exposure.

| e-ISSN: 2319-8753, p-ISSN: 2347-6710| www.ijirset.com | Impact Factor: 8.118|

||Volume 11, Issue 12, December 2022||

| DOI:10.15680/IJIRSET.2022.1112002 |

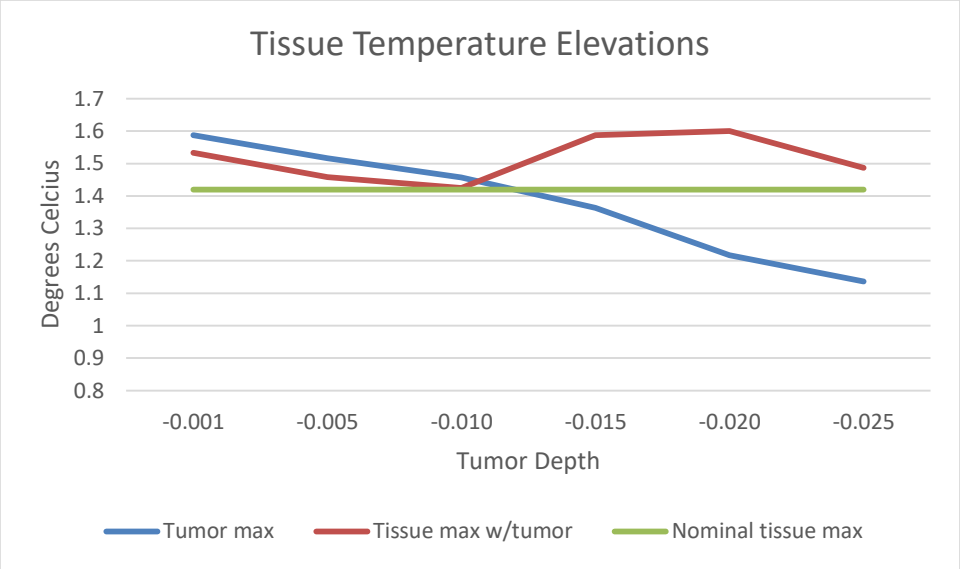

Fig.4. Tissue temperature elevations with changing tumor depth at higher power EM exposure.

The FEM mesh size has been chosen gradually decreasing with the minimum being at the tumor for detailed analysis. As a result, the simulation time has been conservatively prolonged with optimum benefit.

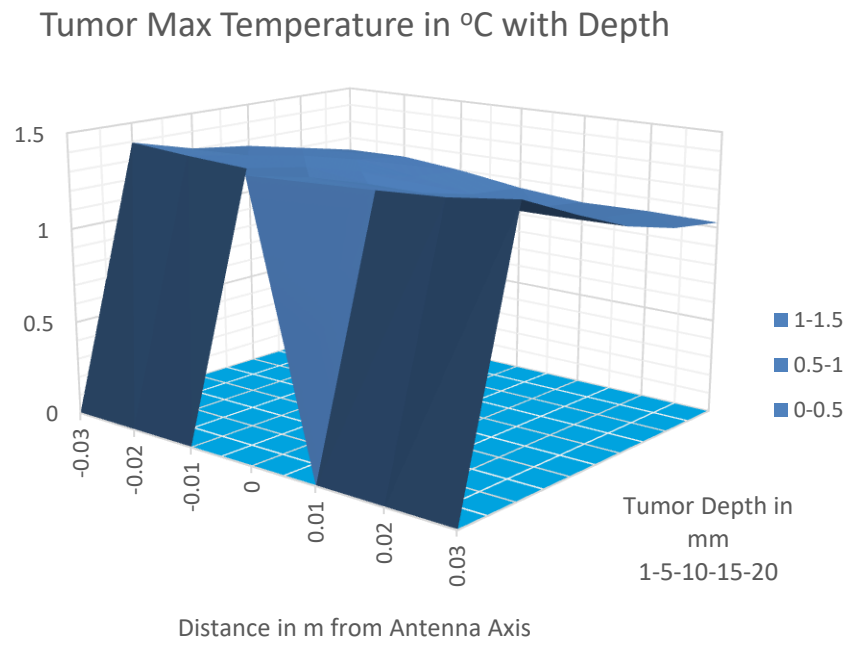

Fig.5. Tumor maximum temperature elevation with depth at lower power EM exposure.

| e-ISSN: 2319-8753, p-ISSN: 2347-6710| www.ijirset.com | Impact Factor: 8.118|

||Volume 11, Issue 12, December 2022||

| DOI:10.15680/IJIRSET.2022.1112002 |

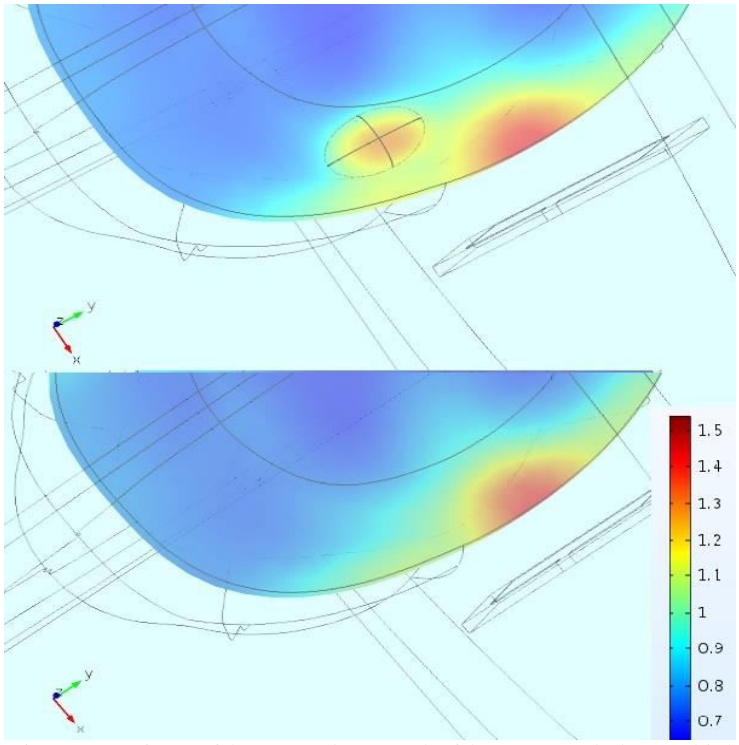

Fig.6. Temperature elevation comparison with tumor above and without tumor below at higher power EM exposure.

The authors have simulated the second model (Fig. 2.) for comparison reasons. Our figures in temperatures were higher both in absolute numbers and in elevations because of metabolic rate definitions compared to Kunter et al [15]. The rather homogenous structure of breast tissue compared to brain and the higher difference in dielectric values of breast tissue and the tumor have made it more visible and detectable as can be seen in Fig. 7.

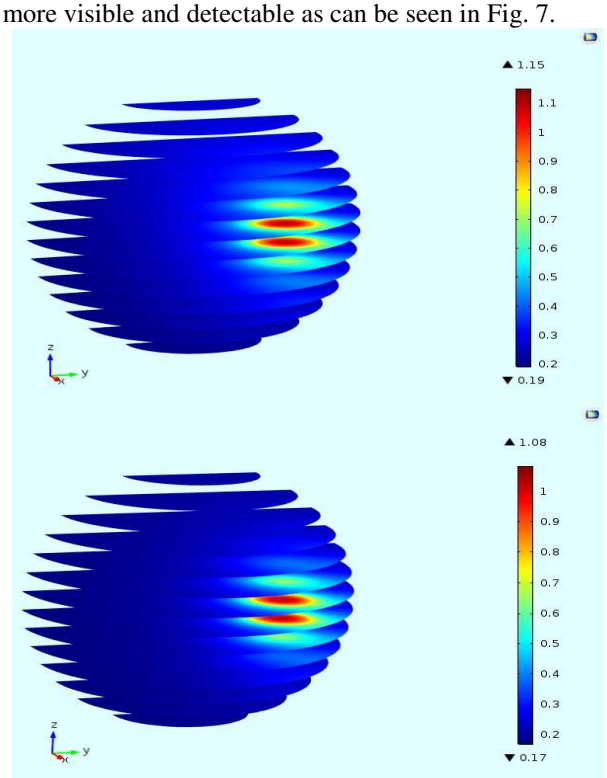

Fig.7. Temperature elevation comparison in breast with tumor with higher power (above) and lower power (below) EM exposure.

| e-ISSN: 2319-8753, p-ISSN: 2347-6710| www.ijirset.com | Impact Factor: 8.118|

||Volume 11, Issue 12, December 2022||

| DOI:10.15680/IJIRSET.2022.1112002 |

In both models, all temperature elevation figures are in alignment with the literature and the powers are within regulations [15, 21, 22].

IV. DISCUSSIONS

The authors have simulated the GBM tumor in IEEE SAR model in model I (Fig. 1) with fine metabolic heat tunings. The GBM tumor has been exposed to EM at 835 MHz. EM radiation at 835 MHz can penetrate the tissue deep enough for dielectric heating, and it is supported by most of the mobile terminals.

The EM exposure heats up both the tissue and the GBM tumor. Since the GBM tumor metabolic heat is higher, and the GBM tumor absorbs more of the EM energy, it conducts the excessive heat to its surroundings. So, when the GBM tumor is closer to surface, its heat sign can be detected by its temperature difference on the surface. But for that, one would need to know the expected temperature elevation from the mobile terminal. This would change from person to person, from terminal to terminal and from one environment to the other. Secondly, the GBM tumor location is not known before hand and the exposure and measurements should trace a path around the head. If the GBM tumor is near the skull, which is not uncommon [11,13], an abnormal temperature rise between 0.1-0.3 oC over nominal case in the GBM tumor and its corresponding skin temperature increase has been observed from simulations. For each simulation, the data could be used to predict a tumor around 30 mm distance both horizontally and vertically to a depth of 20 mm.

A full scan of the head would require minimum seven vertical positions. One would need two horizontal positions at the back of the head in three of the seven vertical positions making it a total of ten scans.

The authors have also simulated the tumor in the breast model in model II (Fig. 2) with fine metabolic heat tunings. The tumor has been exposed to EM at 835 MHz once again. The temperature rise in the second simulations could also be observed. The breast tissue dielectrics has a clear advantage for the dielectric heating with a higher tumor to tissue dielectric ratio. Secondly, the breast is less irregular compared to brain both shape-wise and property-wise. Therefore, the tumor anomaly is very distinct in the breast scenario (Fig. 7).

V. CONCLUSION

The intracranial tumors should be diagnosed in their early stages for successful treatment and recovery [2,3,4,5]. In the GBM case, this is a matter of life and death [11,12]. The COVID-19 pandemic has blocked the access to most of the health services but specially to the advanced medical imaging services. Therefore, a different approach is needed.

The authors have projected a simpler imaging technique using a mobile terminal for the detection of intracranial tumors by means of dielectric heating. The mobile terminal is the source of EM radiation, and it can be coupled with a simple thermometer for result measurements. For the breast tumor case, this has already been proposed with pretty good simulation results [15].

The brain scenario is rather complex, and it requires more scans compared to the breast scenario. The simulation results (Fig. 3-4-5) have shown us that GBM could be detected to a depth of 20 mm. The power seems to be a discriminating factor. For the lower EM power, the temperature elevation relation is quite linear with tumor depth (Fig. 3). As the power increases, the existence of GBM tumor can be detected by the abnormal increase in the normal tissue temperature in the immediate vicinity of the tumor (Fig. 4).

Metabolic rate introduction was critical in getting more realistic results. In the brain scenario, it was critical to tune the nominal temperature of the GBM tumor. In the breast scenario, it was an improvement over the former results with a distinct temperature and visibility advantage [15].

The real-life application will need a simple wearable headset around the head. The scans needed are high in number, but this can be further decreased with the statistics of GBM tumor locations. The usage may still require patience, but it will not violate any social distancing and would not risk the person with an unnecessary Covid-19 infection.

VI. ACKNOWLEDGMENTS

This work is supported by Bogazici University Research Foundation as part of the scientific research project BAP-9860. The authors thank Ozlem SIMSEK (https://orcid.org/0000-0002-7968-1384) for her help.

| e-ISSN: 2319-8753, p-ISSN: 2347-6710| www.ijirset.com | Impact Factor: 8.118|

||Volume 11, Issue 12, December 2022||

| DOI:10.15680/IJIRSET.2022.1112002 |

REFERENCES

[1] World Health Organization (WHO) (https://www.who.int/health-topics/cancer#tab=tab_1)
[2] Yang, Z., Bai, S., Gu, B., Peng, S., Liao, W. and Liu, J., 2015. Radiation-induced brain injury after radiotherapy for brain tumor. Molecular Considerations and Evolving Surgical Management Issues in the Treatment of Patients with a Brain Tumor.
[3] Gupta, K. and Burns, T.C., 2018. Radiation-induced alterations in the recurrent glioblastoma microenvironment: therapeutic implications. Frontiers in oncology, 8, p.503.
[4] Oei, A.L., Vriend, L.E.M., Krawczyk, P.M., Horsman, M.R., Franken, N.A.P. and Crezee, J., 2017. Targeting therapy-resistant cancer stem cells by hyperthermia. International Journal of Hyperthermia, 33(4), pp.419-427.
[5] Repasky, E.A., Evans, S.S. and Dewhirst, M.W., 2013. Temperature matters! And why it should matter to tumor immunologists. Cancer immunology research, 1(4), pp.210-216.
[6] Grauer, O., Jaber, M., Hess, K., Weckesser, M., Schwindt, W., Maring, S., Wölfer, J. and Stummer, W., 2019. Combined intracavitary thermotherapy with iron oxide nanoparticles and radiotherapy as local treatment modality in recurrent glioblastoma patients. Journal of neuro-oncology, 141(1), pp.83-94.
[7] Gupta, R. and Sharma, D., 2020. Manganese-Doped Magnetic Nanoclusters for Hyperthermia and Photothermal Glioblastoma Therapy. ACS Applied Nano Materials, 3(2), pp.2026-2037.
[8] Salehi, A., Paturu, M., Caine, M., Klein, R. and Kim, A.H.,. Laser Therapy Enhances Blood-Brain Barrier and Blood-Tumor Barrier Permeability in a Mouse Model of Glioblastoma. Neurosurgery, 66(Supplement_1), p.nyz310_635.
[9] Benos, L., Spyrou, L.A. and Sarris, I.E., 2019. Development of a new theoretical model for blood-CNTs effective
[10] thermal conductivity pertaining to hyperthermia therapy of glioblastoma multiform. Computer methods and programs in biomedicine, 172, pp.79-85.
[11] Zhou, Y., Zhou, Y., Shingu, T., Feng, L., Chen, Z., Ogasawara, M., Keating, M.J., Kondo, S. and Huang, P., 2011. Metabolic alterations in highly tumorigenic glioblastoma cells preference for hypoxia and high dependency on glycolysis. Journal of Biological Chemistry, 286(37), pp.32843-32853.
[12] National Brain Tumor Society (NBTS-USA) (https://braintumor.org/brain-tumor-information/understanding-brain-tumors/tumor-types/#glioblastoma-multiforme)
[13] Louis, D.N., Perry, A., Reifenberger, G., Von Deimling, A., Figarella-Branger, D., Cavenee, W.K., Ohgaki, H., Wiestler, O.D., Kleihues, P. and Ellison, D.W., 2016. The 2016 World Health Organization classification of tumors of the central nervous system: a summary. Acta neuropathologica, 131(6), pp.803-820.
[14] Cedars Sinai Center (CSC) (https://www.cedars-sinai.edu/Patients/Health-Conditions/Brain-Tumors-and-Brain-Cancer.aspx)
[15] Proescholdt, M.A., Haj, A., Doenitz, C., Brawanski, A., Bomzon, Z. and Hershkovich, H.S., 2019. The dielectric properties of brain tumor tissue.
[16] Kunter, F.C., Gündüz, C. and Seker, S.S., 2018. Temperature Increase and Specific Absorption Rate Distribution in Human Breast from Cell Phone Radiation. Journal of Medical Imaging and Health Informatics, 8(6), pp.1186-1191.

INNO SPACE
SJIF Scientific Journal Impact Factor
Impact Factor: 8.118

doi cross ref

ISSN INTERNATIONAL STANDARD SERIAL NUMBER INDIA

निस्केयर NISCAIR

INTERNATIONAL JOURNAL OF INNOVATIVE RESEARCH

IN SCIENCE | ENGINEERING | TECHNOLOGY

9940 572 462 6381 907 438 ijirset@gmail.com

Scan to save the contact details